Effect of Aluminum Anode Temperature on Growth Rate and Structure of Nanoporous Anodic Alumina

Journal of The Electrochemical Society, 2020 **167** 103506

Effect of Aluminum Anode Temperature on Growth Rate and Structure of Nanoporous Anodic Alumina

Katsiaryna Chernyakova,[1] Boriana Tzaneva,[2,z] Igor Vrublevsky,[3] and Valentin Videkov[2]

[1]*State research institute Center for Physical Sciences and Technology, LT-02300 Vilnius, Lithuania*
[2]*Technical University of Sofia, 1000 Sofia, Bulgaria*
[3]*Belarussian State University of Informatics and Radioelectronics, 220013 Minsk, Belarus*

In the present study, we investigated the effect of an anode temperature on current transient process during porous anodic alumina growth and morphology of the anodic layers. Alumina films were formed in a 0.4 M oxalic acid at a constant voltage mode and electrolyte temperature. The temperature of the Al anode was controlled by thermoelectric Peltier element and varied in the range of 5 °C–60 °C. Surface morphology of both sides of anodic films and their cross-sections were analyzed by scanning electron microscopy (SEM) with subsequent statistical analysis of the SEM images by ImageJ software. It was found that when anode temperature was increased from 5 °C to 50 °C the pores diameter and interpore distance has not changed, but the porous structure became more ordered. According to these results, the rate of chemical dissolution of the barrier layer and pore walls did not depend on the anode temperature. At the anode temperature of 60 °C, pores diameter has increased 1.7 times and there was a distortion of the ordering of porous cells. It was concluded that the temperature difference between the aluminum substrate and electrolyte is an important parameter affecting the formation of ordered structure of nanoporous anodic alumina.
 [DOI: 10.1149/1945-7111/ab9d65]

Manuscript submitted March 28, 2020; revised manuscript received June 9, 2020. Published June 24, 2020.

Temperature is a frequently discussed factor in investigating the growth rate and morphology of self-ordered layers of porous anodic aluminum oxide (AAO). It was found that highly ordered anodic alumina is only obtained at a suitable combination of synthesis conditions such as nature, concentration, and temperature (T_e) of the electrolyte, anodizing current (J_a) and voltage (U_a).[1] To improve the homogeneity of the nanoporous structure, usually, anodizing at low temperatures is recommended (at or below 10 °C), because of the perception that the low rate of AAO growth is favorable for the process of self-organization.[2–4] However, nowadays many authors carry out experiments at elevated electrolyte temperature (at or above 20 °C) to determine the optimal conditions for rapid growth of high-ordered AAO.[5–8] Additionally, the increase in the temperature results in the acceleration of chemical dissolution and in the local burning of the oxide layer.[1,6,9,10] The following thermal effects may occur during aluminum anodizing.

- Joule heating as a result of the current flowing through the electrode and thin film at the bottom of the pores;[10–13]
- exothermic reaction of aluminum oxidation;[10,11]
- an endothermic chemical reaction of aluminum oxide dissolution.[11]

The electrolyte temperature also affected the entire anodizing process, but particularly on the rates of:

- aluminum oxidation by the speed-up of the diffusion of Al^{3+} and O^{2-} ions throughout the barrier layer in the electric field;[14–17]
- circulation of the electrolyte in the pores;[18]
- chemical dissolution of the pore walls[6,7,17] that resulted in the changes of AAO morphology.[13,19,20]

It was also shown that due to the heat generation and low thermal conductivity of the alumina at the Al/oxide interface the temperature is higher than that at the oxide/electrolyte one.[10] Consequently, the temperature on the surface of the film is much lower than that inside the film. Moreover, as aluminum is a good heat conductor, both its thickness and its temperature should also influence the heat balance and from there the growth rate and morphology of porous anodic alumina films. At the same time, the process of heat dissipation during aluminum anodizing is rather complicated and mechanism of its effect on the growth of anodic alumina has not been clearly defined. Although most studies are devoted to the investigation of the influence of electrolyte temperature[6,8,11,21–23] there are several works dealing with the temperature of the anode and its effect on the oxide structure.[9,12,24,25]

Different approaches of influencing the temperature of the anode have been proposed. So, T. Aerts et al. controlled the anode temperature (T_{anode}) using thermostatic holder based on the Peltier effect[25,26] with a thermo-electronic component. In their study aluminum was anodized in aqueous solution of sulfuric acid (with additives of $Al_2(SO_4)_3$) at a constant current mode. However, these conditions allowed the determination of the effect of T_{anode} only on the anode potential and the rate of oxide growth but not on the morphology of the films because of the use of anodizing at a constant current. At the same time, it is known that U_a is one of the key parameters affecting the size of cells, the interpore distance, and pore diameter. Furthermore, from our point of view, large distance between heat-exchanger and aluminum surface (Al foil thickness was 300 μm), as well as, the distance between temperature control module and anodized surface (50 mm) are the points that cause doubts about the efficiency of heat removal and accuracy of its delivery to the work surface. Chowdhury et al.[24] reported the original approach for measuring in situ the temperature of aluminum anode during the self-ordered growth of porous anodic alumina films. They were deposited a Pt thin film as a Resistance Temperature Detector sensor on the backside of aluminum sample with a 12 or 50 μm dielectric alumina layer. The anode temperature was changed by the value of the applied anodizing voltage. However, in these experiments it was impossible to control T_{anode} directly.

In our previous studies,[27,28] it was shown that the thermal conductivity of the substrate influenced dissipation of the Joule heating and hence the rate of oxide layer dissolution and surface morphology of the films. Obviously, it was not possible to measure the temperature directly at the pore bottom, but by varying the anodizing conditions, e.g., anode temperature, one can influence the process of electrochemical oxidation of aluminum, consequently, this should be reflected in the morphology of the films.

So, in the presented work the effect of the Al anode temperature on the structure of the nanoporous anodic alumina films formed in a 0.4 M aqueous solution of oxalic acid at constant voltage mode and

[z]E-mail: borianatz@tu-sofia.bg

electrolyte temperature was studied. The anode temperature was controlled by thermoelectric Peltier element and changed in the range of 5 °C–60 °C. These experiments aimed to show that due to the Joule heat generation, the electrolyte temperature in the electrochemical cell is considerably lower than the one at the pore bottom near the barrier layer and, consequently, the surface morphology of the film in a greater extent should be more dependent on T_e in the pores than on T_e in the electrochemical cell.

Experimental

The high-purity aluminum foil (99.999%, 25 μm thick, AlfaAesar) was used as a starting material. The aluminum specimens were pretreated in a hot solution of 1.5 M NaOH for 15 s, neutralized in 1.0 M H_2SO_4 for 2 min, then carefully rinsed in distilled water and air-dried. The first anodizing was carried out on both sides of the samples in a 0.4 M aqueous solution of oxalic acid at 20 °C at constant voltage of 40 V for 30 min. Then the first layer was removed by etching in the mixture of H_3PO_4 and CrO_3 at 75 °C for 2 h. The second anodizing was done from one side under conditions that were the same as in the first anodizing in the electrochemical cell shown in the Fig. 1. All experiments were carried out at constant electrolyte temperature (T_e) of 20 °C. The anodized area of ca. 2.54 cm^2 was set out by a silicone gasket sealing. The anode temperature was controlled by one or two thermoelectric Peltier elements in the range of 5 °C–60 °C. The second anodizing was carried out for 45 min for $T_{anode} < 40$ °C and until the complete aluminum oxidation for $T_{anode} \geqslant 40$ °C. To determine the rate of oxide layer growth, part of the samples was anodized for 1260 s at different T_{anode}. The anodizing process was controlled by a direct current power supply Voltcraft® Germany (40V/5A). Transient current and voltage values during anodizing were measured and recorded on a computer in real time using two digital multimeters UNI-T UT 71E with data sampling rate of 60 points/min.

Surface morphology of the films and their cross-sections were analyzed by scanning electron microscopy (SEM) on a LEO DSM 982 (Germany) with subsequent statistical analysis of the images by ImageJ software using the procedure described in Refs. 27, 28. It should be noted that pore diameter (d_{pore}) was determined using the top view of the films, at the same time, an interpore distance (D_{inter}) was calculated using bottom view, as the top view possessed the structure of the initiated Al surface (after the first anodizing) and it was difficult to evaluate the accuracy of the obtained results.

Results and Discussion

Effect of anode temperature on the current transient processes during porous anodic alumina formation.—At $T_{anode} \geqslant 40$ °C in current transients one can distinguish three stages shown in Fig. 2 for maximal T_{anode} dependency:

- Stage I (inset in Fig. 2) is the initial stage at which initial anodizing current is very high, then it drops sharply and after that slightly increases, reaching a steady-state value;
- Stage II of the porous oxide growth corresponds to the constant average value of J_a;
- Stage III is the final stage at which J_a gradually decreases and the anodizing process ends.

It should be noted that each of the three stages takes a different time at different T_{anode} due to the different rates of oxide growth. Therefore, at $T_{anode} \leqslant 30$ °C the process was carried out for 45 min and stage III was not achieved because of very slow oxide growth. At $T_{anode} = 40$ °C–60 °C, within the same time, the aluminum foil was oxidized completely and linear decrease in the anodic current density could be observed as a result of the reduction of the aluminum surface due to its local exhaustion (Fig. 2). Considering the initial surface roughness, thickness of aluminum foil (less than 30 μm) and its pretreatment without polishing, we suggest that the observed effects are driven by irregularities in the thickness resulting

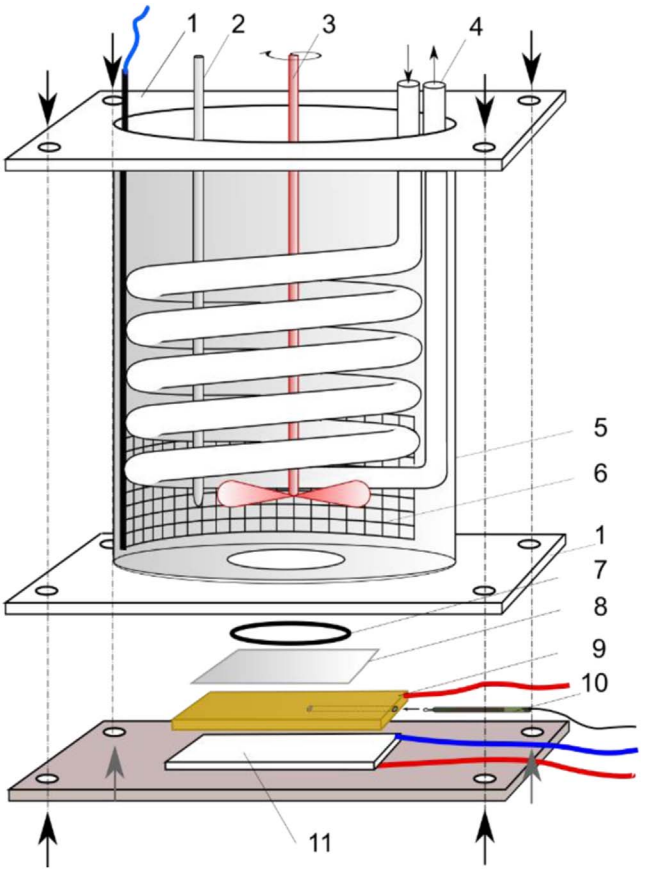

Figure 1. Schematic representation of the electrode temperature control system. 1—Teflon holders; 2—temperature probe I; 3—mechanical stirrer; 4—glass serpentine heat exchanger; 5—glass cell; 6—Pt counter electrode; 7—silicone gasket sealing; 8—aluminum foil; 9—brass plate with connector to (+) pole; 10—temperature probe II; 11—Peltier module with radiator and temperature probe III.

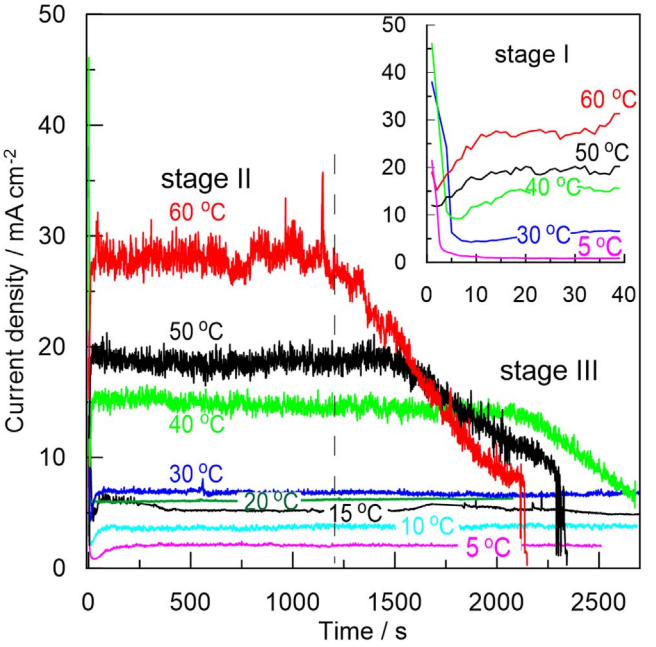

Figure 2. Current transients for porous anodic alumina formation at different anode temperatures of 5 °C–60 °C in a 0.4 M oxalic acid solution (20 °C). Inset shows the initial stages of the anodic alumina formation.

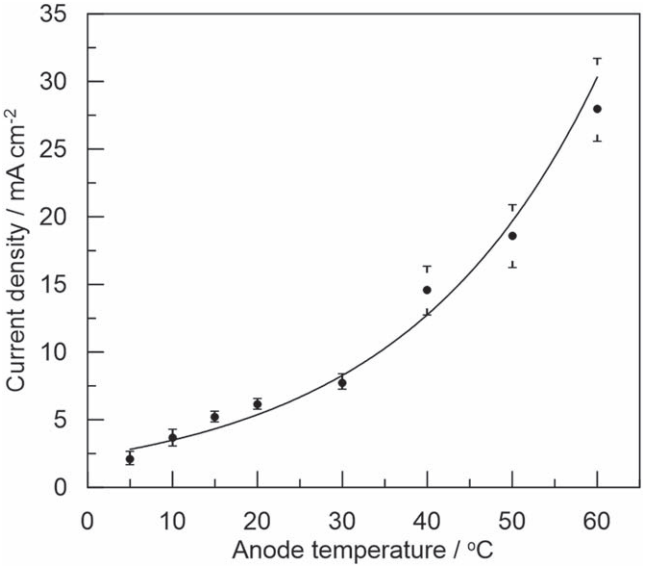

Figure 3. Variations in the average current density (●), maximal (˙) and minimal (˙) values of oscillations during aluminum steady-state anodizing in a 0.4 M oxalic acid (20 °C) at 40 V as function of the anode temperature.

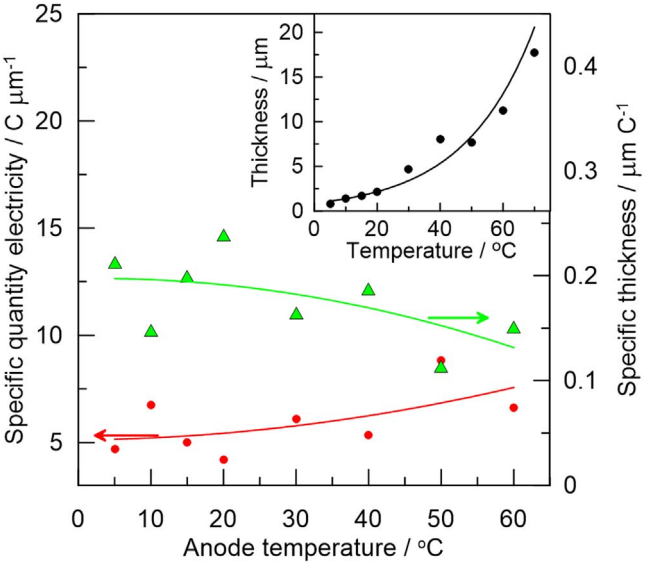

Figure 4. The effect of anode temperature on specific quantity electricity (red points) and specific thickness of oxide layer (green triangles). Inset: Variation in the thickness of anodic layers obtained for 1260 s as function of the anode temperature.

in spatially variable rates of heat and mass transfer which cannot be avoided. In this respect, all subsequent calculations were made without the data obtained on Stage III.

As can be seen from the inset in Fig. 2, at $T_{anode} \leqslant 40$ °C during the initial stage anodizing current sharply drops in 5–7 s, so it decreases 4–5 times comparing to the initial value. In the anode temperature range of 5 °C–40 °C with increasing T_{anode} the initial value of J_a increases, reaching its maximum of 47 mA cm^{-2} at $T_{anode} = 40$ °C. This is explained by the strong influence of temperature on the rate of both chemical dissolution of the natural passive layer on the aluminum surface and the electrochemical process.[1,29] At 5 °C–30 °C the initial anodizing process before the start of pore formation (the decrease in current density) take about 1 min, but at $T_{anode} = 40$ °C this period is shortened and J_a reaches a minimum value of 8 s. At anode temperatures of 50 °C–60 °C, in the current transient curves the current drop is absent in the stage I (the inset in Fig. 2), only gradual growth of J_a by 5–10 mA cm^{-2} s^{-1} with subsequent reaching of a steady-state value is observed. That can be explained by the speed-up of the formation of Al^{3+} ions at higher anode temperatures and a low rate of chemical dissolution of aluminum oxide at a rather low electrolyte temperature. Very similar results with increased electrolyte temperatures were obtained by Sulka and Stepniowski.[15]

In the steady-state of porous oxide growth, the average values of J_a do not change significantly (Fig. 2, stage II), indicating kinetic control of the process.[8] However, rise in T_{anode} increases the amplitude of J_a oscillations from 0.3 mA cm^{-1} at 5 °C to more than 3 mA cm^{-1} at 60 °C and this indicates instability of the heat dissipation process at $T_{anode} \geqslant 40$ °C. Therefore, to determine the dependence of J_a on the T_{anode} during stage II, we calculated the arithmetic mean of the J_a for each substrate temperature. At the steady-state of oxide growth, the current density exponentially rises with increase in T_{anode} (solid line in Fig. 3) and can be described by the following equation:

$$J_a = 2.26e^{0.04T_{anode}} \quad [1]$$

where J_a is anodic current density in mA cm^{-2} and T_{anode} is the anode temperature in °C.

Theoretically, if time is a constant, the thickness of the oxide layer formed at each T_{anode} should be proportional the growth rate of alumina expressed through the density of anodizing current. To verify this statement with respect to AAO growth, the oxide thickness (h) was measured in μm by SEM images of the cross-sections of the oxide layers obtained at different T_{anode} during the same period of anodizing (1260 s) (inset in Fig. 4). Indeed, the thickness also increases exponentially with temperature:

$$h = 0.88e^{0.04T_{anode}} \quad [2]$$

where T_{anode} is the anode temperature in °C.

The factor multiplied T_{anode} in exponential function argument remains the same as in Eq. 1, but the coefficient before the exponential function is lower. That indicates that the thickness increases more slowly with increasing temperature relative to the current density.

Practically, the dependence of J_a on the anodizing time provides only indirect information on the rate of the alumina formation, as the barrier layer possesses high thermal resistance and part of the electrical energy converts to thermal energy that consequently speeds-up alumina dissolution. To exclude the loss of electrical energy as heat dissipation and chemical dissolution of oxide, the specific quantity of electricity (Q_h) was calculated as the quantity of electricity required to form the layer of anodic alumina with a thickness of 1 μm using to the following equation:

$$Q_h = \frac{Q}{h} = \frac{1}{h}\int_0^t I(t)\,dt \ [\mathrm{C}/\mu\mathrm{m}] \quad [3]$$

where Q is the quantity of electricity calculated using transient current passed through the system over the time $t \in [0, 1260]$ s. The specific quantity of electricity slightly increases with the anode temperature and accordingly its reciprocal value of specific thickness of the anodic alumina layer decreases (Fig. 4). Therefore, it can be assumed that the rate of its chemical dissolution weakly increases. However, the anisotropy of porous alumina dissolution should be considered, which means that pore walls dissolve faster than the bulk alumina does. So, to evaluate the effect of anode temperature on the rate of chemical dissolution of alumina and electrochemical oxidation of aluminum we should also study the morphology of the films formed at different anode temperatures.

Effect of anode temperature on the structure of nanoporous anodic alumina.—Usually, during aluminum anodizing the anode temperature rises as a result of current flow at high anode potentials.

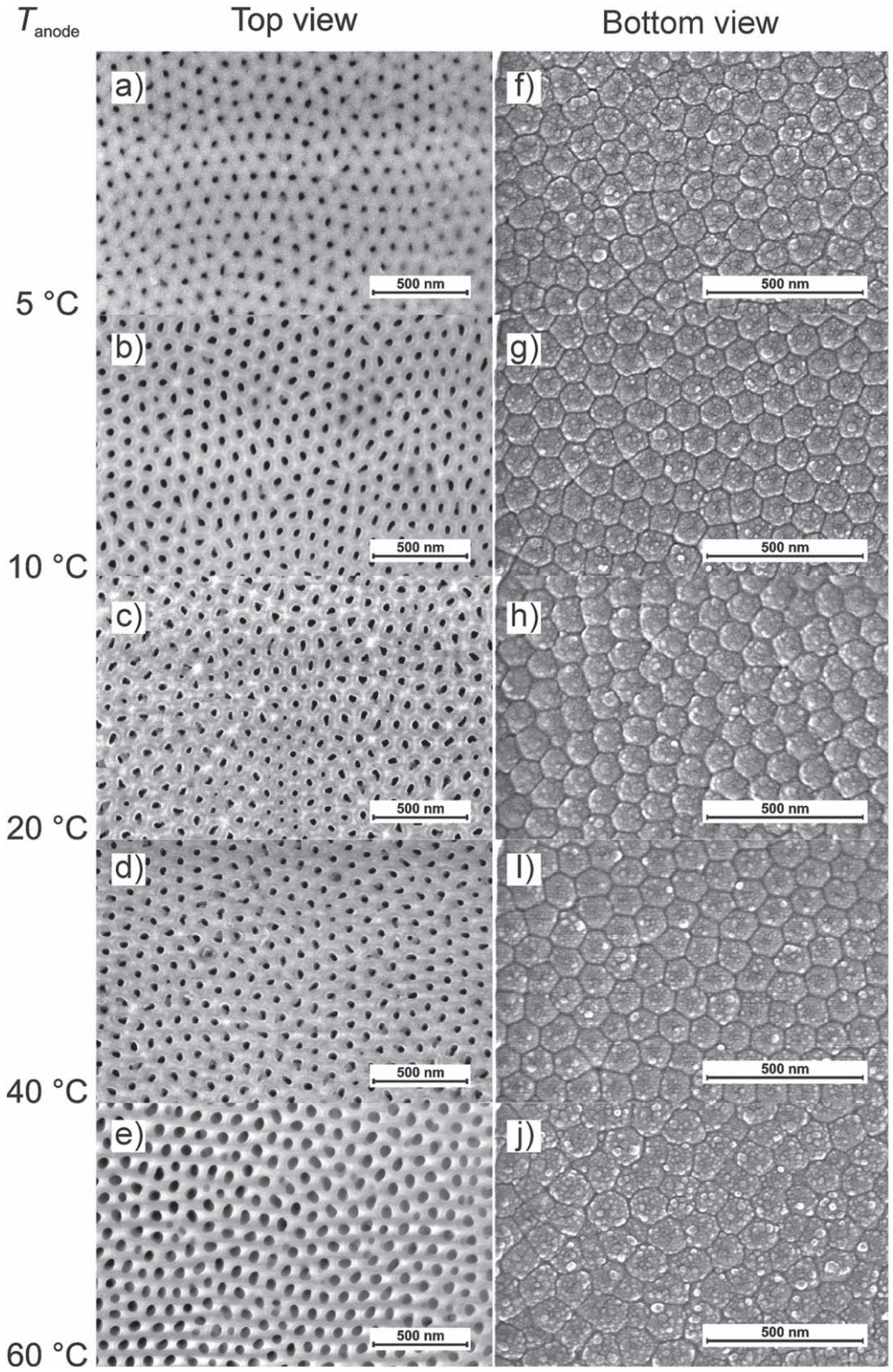

Figure 5. SEM images of the top (a)–(e) and bottom (f)–(j) view of self-ordering of anodic alumina membrane formed at different anode temperatures 5 °C–60 °C, 40 V in a 0.4 M oxalic acid solution (20 °C).

At these modes, the so-called burnout effect takes place and disorder of the oxide layer structure increases.[30,31] Each new portion of electrolyte reaching the pore bottom participates both in the formation of new layers of anodic alumina and in the dissolution of the barrier layer, which determines the thickness of this layer.[1] At the same time, due to Joule heat generation the temperature of electrolyte portion leaving the pore is higher than T_e, therefore, the pore walls dissolve faster as the process progresses, and, consequently, the size and shape of the pores should change. This effect should be the strongest at the pore bottom where the electrolyte temperature is maximal. Despite these expectations, when T_{anode} was increased from 5 °C to 50 °C neither d_{pore} nor D_{inter} has significantly changed (Figs. 5 and 6). In the mentioned temperature range, d_{pore} is maintained at 31 nm and D_{inter} is 104–111 nm. Therefore, the rate of

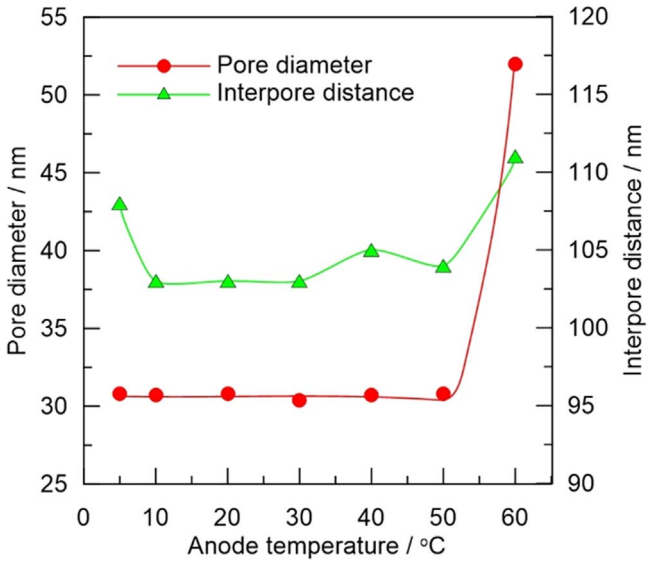

Figure 6. Variations in the average pore diameter and average interpore distance of self-ordered anodic alumina films obtained in a 0.4 M oxalic acid (20 °C) at 40 V as function of the anode temperature.

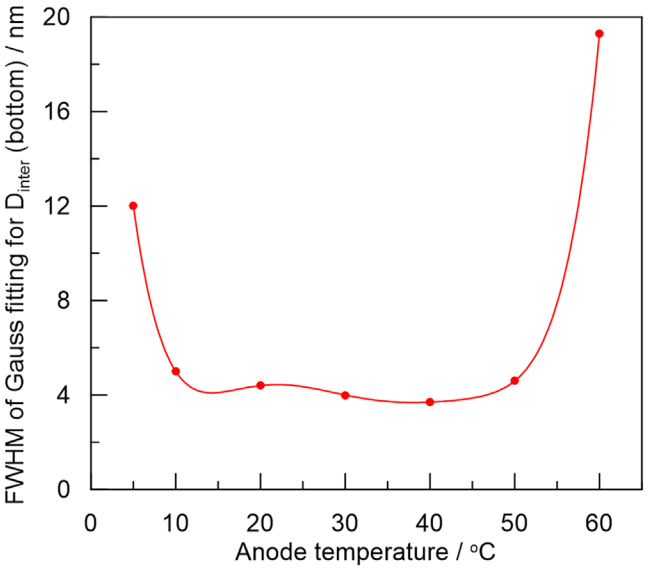

Figure 7. Full width at half maximum of the Gauss curves for D_{inter} as a function of anode temperature for the anodic alumina films formed in a 0.4 M oxalic acid (20 °C) at 40 V.

chemical dissolution of the barrier layer and pore walls was constant and did not depend on the anode temperature. That indicates that the temperature of the electrolyte leaving the pores was higher than 50 °C. However, at T_{anode} = 60 °C d_{pore} increases to 52 nm (in 1.7 times) at the same time, the uniformity in the ordering and the size of the cells was destroyed (Fig. 5).

To calculate d_{pore} and D_{inter} the SEM images were processed by ImageJ. So, we plotted the curves of d_{pore} and D_{inter} size distribution and fitted by Gaussian curves.[27,28] Then a full width at half maximum (FWHM) of the Gauss curves for D_{inter} obtained at each T_{anode} were determined. In this way, the size disturbance of the cells was characterized (Fig. 7). Initially FWHM decreases from 12 (at T_{anode} = 5 °C) to 4–5 nm (T_{anode} = 20 °C–50 °C) and then increases again to almost 20 nm (at T_{anode} = 60 °C). As one can see, at different anode temperatures both d_{pore} and FWHM changed significantly while the average D_{inter} varies slightly (Figs. 6 and 7). That confirms the model for coupled electrical migration and stress-driven transport of oxide toward the pore walls during aluminum anodizing.[32–36] According to this theory, growth of the anodic film at the barrier region of the porous film is accompanied by a displacement of film material from the barrier layer towards the cell walls in such a way that the interpore distance is maintained along the entire thickness of the oxide.

Therefore, the entire range of anode temperatures can be divided into three regions depending on the ratio of T_{anode} to T_e as follows:

Region 1: 5 °C $\leqslant T_{anode} <$ 20 °C (Fig. 8a), in this region $T_e > T_{anode}$, therefore, some part of the heat from the reaction of alumina formation and from the electrolyte was transferred to the substrate. Therefore, the temperature of electrolyte leaving the pores was not much higher than 20 °C, i.e., diameter of pores and cells depended on the temperature of the electrolyte flow. At the lowest temperature, this supercooling effect at the Al/AAO interface was maximum and, as a result, the oxide structure was disordered, FWHM of the Gauss curves for D_{inter} was about 12 nm (Fig. 7), despite the fact that the average value of d_{pore} was constant;

Region 2: 20 °C $\leqslant T_{anode} \leqslant$ 50 °C (Fig. 8b), in this region $T_e \leqslant T_{anode}$. In that case, more and more parts of the heat from the anodization process were transferred to the electrolyte flow leaving the pores. Its temperature was even higher than that of the bulk electrolyte. The substrate temperature was probably still lower than that in the barrier layer due to the Joule heating. This complies with the results obtained by Schneider et al. which show an increase in the aluminum substrate temperature more than 55 °C compared to that of the bulk electrolyte.[10] The resulting films were highly ordered, FWHM of the Gauss curves for D_{inter} was constant and equal to 4 nm, d_{pore} was also independent on the T_{anode} (Figs. 6 and 7). Therefore, it can be assumed that the temperature of the electrolyte in the pores does not significantly depend on that of the substrate. Moreover, the average values of the current density J_a did not change during anodizing process even when relatively thick alumina (thicker than 15 μm) was formed. One could expect that with increasing thickness of anodic alumina layer, the heat transfer from anode to the electrolyte would be impeded and at the pore bottom T_e would grow increasing J_a. However, the results did not demonstrate such behavior of anodizing current (Fig. 2);

Region 3: $T_{anode} \geqslant$ 60 °C (Fig. 8c), $T_{anode} >> T_e$ and higher than the temperature of electrolyte leaving the pores, therefore, electrolyte can be additionally heated by the anode. The temperature gradient between the two alumina sides was maximal and this was reflected in an increase in the circulation rate of the electrolyte in the pores. As a result, the increase in the rate of chemical dissolution of pore walls was observed. Moreover, SEM results also show that the cells were disordered and FWHM of the Gauss curves for D_{inter} rises to 20 nm (Fig. 7).

According to SEM observations the pore diameter does not change over the entire length of the channels at the all studied T_{anode}. As an example, Fig. 8d presents the cross-sectional SEM image at the bottom and at the mouth of the pores for anodic film obtained at 15 °C. Therefore, it can be assumed that the film structure self-regulates as a result of establishing equilibrium along the entire length of the pore channels due to cooling of the electrolyte when it moves from the bottom to the pore mouth. If the electrolyte leaving the pores remained hot, the pores would have to be conical rather than cylindrical due to the longer dissolution of the walls near the alumina/electrolyte interface.[13] However, this was not observed and all pores were cylindrical even with a large thickness of the anode film. It is likely that maintaining equilibrium between the processes that accelerate and inhibit the dissolution of pore walls takes place only at temperatures from 20 to 50 °C, and, therefore, the structure manages to self-regulate and a high degree of ordering of the cell structure is preserved. Compared to our results at T_e = 20 °C, those obtained by other authors at higher electrolyte temperatures also show accelerated pore walls dissolution at 30 °C.[6,15] At $T_{anode} \geqslant$ 60 °C, an imbalance between the rate of chemical dissolution and the rate of formation of new oxide layers occurs. As a result, with increasing thickness, the structure of the porous alumina becomes

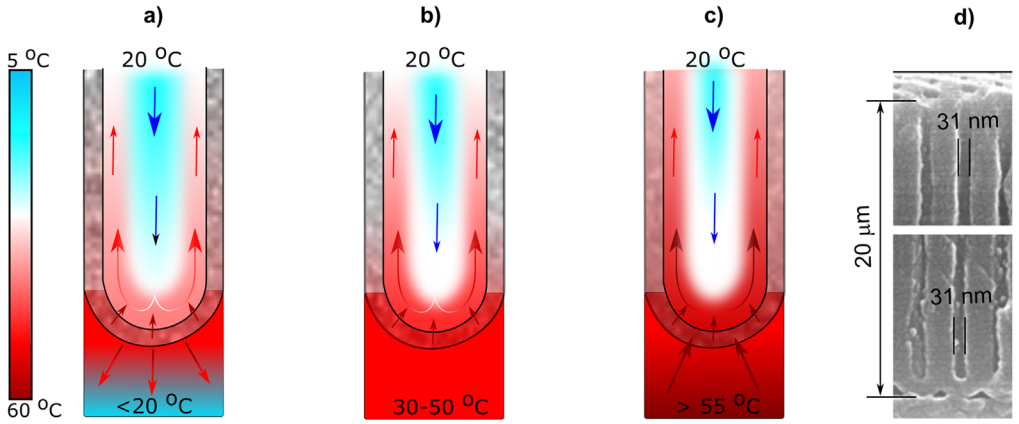

Figure 8. Schematic illustration of heat flow during anodizing process at different anode temperature: (a) supercooling, (b) low temperature heating and (c) overheating; (d) cross-sectional SEM image at the bottom and the mouth of the pores for anodic film obtained at 15 °C.

more disordered According to A.P. Leontiev et al. at high electrolyte temperature and AAO thickness above a certain critical value (only 5 μm at 50 °C) the kinetically controlled anodizing switches to the mixed regime destroying the hexagonal pore ordering.[8] However, it should be noted that according to our results at $T_{anode} = 50$ °C the thickness of the resulting oxide layer was 20 μm and the degree of pore ordering was fairly high (FWHM = 4 nm).

Therefore, it could be assumed that the condition for obtaining a high-ordered structure is rather a suitable optimal temperature difference between the aluminum substrate and electrolyte than a fixed low electrolyte temperature. This assumption supports the convective mechanism proposed by Pashchanka and Schneider to explain self-organization on nanoscale.[18] This optimal temperature difference is necessary to ensure a good circulation of the electrolyte inside the pores. Thus, a high degree of ordering can also be achieved at a higher electrolyte temperature (e.g., 20 °C), but at slightly elevated anode temperature. These conditions also allow for a significant acceleration of the anodizing process and the formation of a high-structured layer in a short time.

Conclusions

It was established that the average values of J_a and oxide thickness over steady-state region increase exponentially with the anode temperatures rise, but the specific quantity of electricity did not depend on the anode temperature significantly. It has been suggested that depending on the aluminum substrate temperature, the heat flow during anodizing process affects the electrolyte temperature at the pore bottom and thus influences the rate of chemical oxide dissolution and electrolyte circulation to formation of porous structure of anodic films.

It was shown that at anode temperatures ranging from 20 to 50 °C neither d_{pore} nor D_{inter} has changed (d_{pore} is 31 nm and D_{inter} is 104 nm) indicating that the temperature of the electrolyte leaving the pores was higher than 50 °C as results of Joule heating.

A distortion of the cells ordering was observed both at supercooling (at 5 °C) and at overheating (at 60 °C) of aluminum substrate.

It was suggested for the obtaining of anodic alumina with high degree of ordering, optimal temperature gradient from the aluminum substrate to electrolyte is needed rather than a fixed low electrolyte temperature. Thus, a high growth rate of nanostructured AAO can also be achieved at a higher electrolyte temperature, but at slightly elevated anode temperature.

Acknowledgments

The authors express their gratitude for the financial support by the research project КП-06-H29/1, funded by the National Science Found (Bulgaria).

ORCID

Boriana Tzaneva https://orcid.org/0000-0002-3289-9124

References

1. W. Lee and S.-J. Park, *Chem. Rev.*, **114**, 7487 (2014).
2. O. Jessensky, F. Müller, and U. Gösele, *J. Electrochem. Soc.*, **145**, 3735 (1998).
3. S. Z. Chu, K. Wada, S. Inoue, and S. Todoroki, *J. Electrochem. Soc.*, **149**, B321 (2002).
4. S. Shingubara, K. Morimoto, H. Sakaue, and T. Takahagi, *Electrochem. Solid-State Lett.*, **7**, E15 (2004).
5. O. Nishinaga, T. Kikuchi, S. Natsui, and R. O. Suzuki, *Sci. Rep.*, **3**, 2748 (2013).
6. F. A. Bruera, G. R. Kramer, M. L. Vera, and A. E. Ares, *Surf. Interfaces*, **18**, 100448 (2020).
7. L. Zaraska, W. J. Stepniowski, E. Ciepiela, and G. D. Sulka, *Thin Solid Films*, **534**, 155 (2013).
8. A. P. Leontiev, I. V. Roslyakov, and K. S. Napolskii, *Electrochim. Acta*, **319**, 88 (2019).
9. I. De Graeve, H. Terryn, and G. E. Thompson, *J. Appl. Electrochem.*, **32**, 73 (2002).
10. M. Schneider, C. Lämmel, C. Heubner, and A. Michaelis, *Mater. Corros.*, **64**, 60 (2013).
11. M. Nagayama and K. Tamura, *Electrochim. Acta*, **13**, 1773 (1968).
12. I. De Graeve, H. Terryn, and G. E. Thompson, *J. Electrochem. Soc.*, **150**, B158 (2003).
13. T. Aerts, T. Dimogerontakis, I. De Graeve, J. Fransaer, and H. Terryn, *Surf. Coat. Technol.*, **201**, 7310 (2007).
14. A. Baron-Wiecheć, P. Skeldon, J. J. Ganem, I. C. Vickridge, and G. E. Thompson, *J. Electrochem. Soc.*, **159**, C583 (2012).
15. G. D. Sulka and W. J. Stepniowski, *Electrochim. Acta*, **54**, 3683 (2009).
16. S. Stojadinović, N. Tadić, N. Radić, B. Stojadinović, B. Grbić, and R. Vasilić, *Surf. Coat. Technol.*, **276**, 573 (2015).
17. G. E. Thompson, *Thin Solid Films*, **297**, 192 (1997).
18. M. Pashchanka and J. J. Schneider, *J. Mater. Chem.*, **21**, 18761 (2011).
19. T. Kikuchi, O. Nishinaga, D. Nakajima, J. Kawashima, S. Natsui, N. Sakaguchi, and R. O. Suzuki, *Sci. Rep.*, **4**, 7411 (2014).
20. L. C. François, A. Laurent, and L. Datas, *Mater. Charact.*, **61**, 283 (2010).
21. L. Ba and W. S. Li, *J. Phys. D: Appl. Phys.*, **33**, 2527 (2000).
22. Y. Goueffon, C. Mabru, M. Labarrиre, L. Arurault, C. Tonon, and P. Guigue, *Surf. Coat. Technol.*, **205**, 2643 (2010).
23. Y. Ma et al., *J. Electrochem. Soc.*, **165**, E311 (2018).
24. P. Chowdhury, A. N. Thomas, M. Sharma, and H. C. Barshilia, *Electrochim. Acta*, **115**, 657 (2014).
25. T. Aerts, J. B. Jorcin, I. De Graeve, and H. Terryn, *Electrochim. Acta*, **55**, 3957 (2010).
26. T. Aerts, I. De Graeve, and H. Terryn, *Electrochem. Commun.*, **11**, 2292 (2009).
27. I. Vrublevsky, A. Ispas, K. Chernyakova, and A. Bund, *J. Solid State Electrochem.*, **20**, 2765 (2016).
28. K. Chernyakova, I. Vrublevsky, V. Klimas, and A. Jagminas, *J. Electrochem. Soc.*, **165**, E289 (2018).
29. M. M. Lohrengel, *Mater. Sci. Eng.*, **R11**, 243 (1993).
30. J. M. Montero-Moreno, M. Sarret, and C. Müller, *Microporous Mesoporous Mater.*, **136**, 68 (2010).
31. T. Aerts, I. D. Graeve, and H. Terryn, *Electrochim. Acta*, **54**, 270 (2008).
32. S. J. Garcia-Vergara, P. Skeldon, G. E. Thompson, and H. Habazaki, *Electrochim. Acta*, **52**, 681 (2006).
33. S. J. Garcia-Vergara, L. Iglesias-Rubianes, C. E. Blanco-Pinzon, P. Skeldon, G. E. Thompson, and P. Campestrini, *Proc. R. Soc. London, Ser. A*, **462**, 2345 (2006).
34. J. E. Houser and K. R. Hebert, *Nat. Mater.*, **8**, 415 (2009).
35. K. R. Hebert and P. Mishra, *J. Electrochem. Soc.*, **165**, E737 (2018).
36. K. R. Hebert and P. Mishra, *J. Electrochem. Soc.*, **165**, E744 (2018).